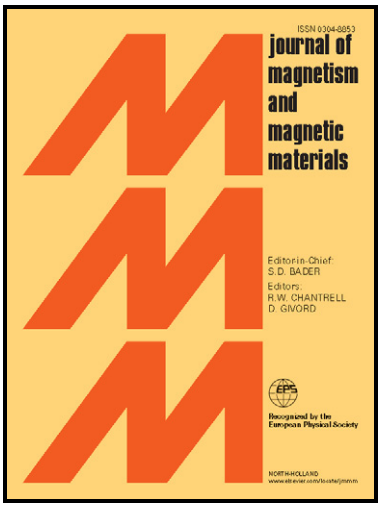

www.elsevier.com/locate/jmmm

Intra-well relaxation process in magnetic fluids subjected to strong polarising fields

C.N. Marin, P.C. Fannin, I. Mălăescu, P. Barvinschi, A. Ercuţa

PII: S0304-8853(11)00557-9
DOI: doi:10.1016/j.jmmm.2011.08.011
Reference: MAGMA 57061

To appear in: *Journal of Magnetism and Magnetic Materials*

Received date: 2 June 2011
Accepted date: 5 August 2011

Cite this article as: C.N. Marin, P.C. Fannin, I. Mălăescu, P. Barvinschi and A. Ercuţa, Intra-well relaxation process in magnetic fluids subjected to strong polarising fields, *Journal of Magnetism and Magnetic Materials*, doi:10.1016/j.jmmm.2011.08.011

Intra-well relaxation process in magnetic fluids subjected to strong polarising fields

C. N. Marin [1, 1]*, P. C. Fannin [2], I. Mălăescu [1], P. Barvinschi [1], A. Ercuța [1]

[1] *West University of Timisoara, Faculty of Physics, B-dul V. Parvan, no. 4, Timisoara, 300223, Romania*

[2] *Department of Electronic and Electrical Engineering, Trinity College, Dublin 2, Ireland*

Abstract

We report on the frequency and field dependent complex magnetic susceptibility measurements of a kerosene-based magnetic fluid with iron oxide nanoparticles, stabilized with oleic acid, in the frequency range 0.1 – 6 GHz and over the polarising field range of 0 – 168.4 kA/m.

By increasing polarizing field, *H*, a subsidiary loss-peak clearly occurs in the vicinity of the ferromagnetic resonance peak, from which it remains distinct even in strong polarising fields of 168.4 kA/m. This is in contrast to other reported cases in which the intra-well relaxation process is manifested only as a shoulder of the resonance peak and which vanishes in polarising fields larger that 100 kA/m.

The results of the XRD analysis connected to the anisotropy field results confirm that the investigated sample contains particles of magnetite and of the tetragonal phase of maghemite.

Taking into account the characteristics of our sample, the theoretical analysis revealed that the intra-well relaxation process of the small particles of the tetragonal phase of maghemite may be responsible for the subsidiary loss peak of the investigated magnetic fluid.

PACS number(s): 47.65.Cb, 75.40.Gb, 76.50.+g

Keywords: magnetic fluids; dynamic susceptibility; ferromagnetic resonance.

*Author to whom the correspondence should be addressed. E-mail address: cmarin@physics.uvt.ro

1. Introduction

The magnetic relaxation in nanoparticle systems is a widely investigated topic, which has attracted the interest of scientists both from applicative perspectives and from a fundamental point of view.

The first accurate theoretical results on the magnetic relaxation in a system of non-interacting single-domain particles with uniaxial anisotropy is due to W. F. Brown [1]. He derived the Fokker-Planck equation of the system in the presence of a polarising field, H, applied parallel to the uniaxial anisotropy axes of the particles and then solved the corresponding Sturm-Liouville equation for two limiting cases of energy barrier σ, which is a ratio of anisotropy energy to thermal energy. The two cases were: i) low energy barrier and small polarising field and ii) high energy barrier [1]. In his computations, W. F. Brown assumed that the magnetic relaxation was dominated by a single relaxation mode which was determined by the lowest non-vanishing eigenvalue of the Sturm-Liouvile equation.

Coffey et al. [2] tested theoretically the validity of this assumption and arrived at the conclusion that it is correct only in the case of zero polarising field. For values of the ratio $h=H/H_A$ (where H_A is the anisotropy field) larger than 0.15, the higher order eigenvalues of the Sturm-Liouville equation become important in the magnetic relaxation process [2]. The lowest non-vanishing eigenvalue of the Sturm-Liouvile equation is correlated to the over-barrier relaxation process (also known as the Néel relaxation process) and the higher order eigenvalues of the Sturm-Liouville equation are associated to the intra-well relaxation process [3].

The first experimental evidences on the existence of the intra-well relaxation process have been reported in the case of magnetic fluids with magnetite particles [4], where the intra-well relaxation process manifested as a shoulder in the ferromagnetic resonance absorption peak of $\chi''(\omega, H)$. However, in Ref. [4], this shoulder disappeared for values of H larger than 100 kA/m. A similar behaviour of the frequency and polarising field dependence of the susceptibility of magnetic fluids can be seen in Refs. [5-7].

In this paper we report on the intra-well relaxation process in a magnetic fluid subjected to strong polarising fields. Unlike other reported data, mentioned above (Refs.

[4 -7]), here the intra-well relaxation peak remains distinct from the resonance peak even for values of H equal to 168.4 kA/m. To explain this phenomenon, a theoretical analysis is presented, which, taking into account the characteristics of the sample, reveals that the intra-well relaxation process of the small particles of the tetragonal phase of maghemite may be responsible for the subsidiary loss-peak.

2. Theoretical considerations

$\chi(\omega,H)$ of a magnetic fluid may be written in terms of its parallel, $\chi_{\parallel}(\omega,H)$ and perpendicular, $\chi_{\perp}(\omega,H)$ components [8], with

$$\chi(\omega,H)=\frac{1}{3}\left[\chi_{\parallel}(\omega,H)+2\chi_{\perp}(\omega,H)\right] \tag{1}$$

The contribution of the over-barrier and intra-well relaxation processes to the $\chi_{\parallel}(\omega,H)$ component of an assembly of non-interacting single-domain particles with uniaxial anisotropy may be expressed by means of the normalized autocorrelation function, $C_{\parallel}(t,H)$ [9]:

$$\begin{aligned}&\chi_{\parallel}(\omega,H)=\chi'_{\parallel}(\omega,H)-i\chi''_{\parallel}(\omega,H)=\\&=\chi_{\parallel}(0,H)\left[1-i\omega\int_0^{\infty}C_{\parallel}(t,H)\exp(-i\omega t)\,dt\right]\end{aligned} \tag{2}$$

In Eq. (2) $\chi'_{\parallel}(\omega,H)$ and $\chi''_{\parallel}(\omega,H)$ are the real and the imaginary parts of the parallel complex magnetic susceptibility and $\chi_{\parallel}(0,H)$ is the parallel static magnetic susceptibility, which can be expressed as [6]:

$$\chi_{\parallel}(0,H)=\frac{v^2M_S^2n}{k_BT}\left[\frac{1+2\langle P_2\rangle_0}{3}-\langle P_1\rangle_0^2\right] \tag{3}$$

where, v is the magnetic volume of a particle, M_S is the spontaneous magnetization of the material of the particles, T is the temperature of the system, k_B is Boltzmann's constant and n is the particle concentration. Also, $\langle P_1 \rangle_0 = \langle P_1(\cos\theta) \rangle_0$ and $\langle P_2 \rangle_0 = \langle P_2(\cos\theta) \rangle_0$ are the averaged Legendre polynomials of the polar angle cosines corresponding to the magnetic moment of the particle. Assuming that the polarising field is parallel both to the anisotropy axis and to the oz axis, $\langle P_1 \rangle_0$ and $\langle P_2 \rangle_0$ may be expressed by means of the parameters $\xi = \frac{vHM_S}{k_B T}$ and $\sigma = \frac{Kv}{k_B T}$ (where K is the uniaxial anisotropy constant) as follows [6]:

$$\langle P_1 \rangle_0 = \frac{\exp(\sigma)\sinh(\xi)}{\sigma Z} - \frac{\xi}{2\sigma} \tag{4}$$

$$\langle P_2 \rangle_0 = \frac{3\exp(\sigma)}{2\sigma Z}\left[\cosh(\xi) - \frac{\xi}{2\sigma}\sinh(\xi)\right] + \frac{3\xi^2}{8\sigma^2} - \frac{3}{4\sigma} - \frac{1}{2} \tag{5}$$

with

$$Z = \int_{-1}^{1} \exp\left(\sigma x^2 + \xi x\right) dx \tag{6}$$

Assuming that the autocorrelation function, $C_{\parallel}(t, H)$ is determined only by the over-barrier and intra-well relaxation processes, it can be written as:

$$C_{\parallel}(t, H) = \Delta_1 \exp(-\lambda_1 t) + (1 - \Delta_1)\exp\left(-\frac{t}{\tau_W}\right) \tag{7}$$

In Eq. (7) τ_W is the intra-well relaxation time and Δ_1 is the weight of the over-barrier relaxation mode, corresponding to the lowest eigenvalue of the Sturm-Liouville equation, λ_1. Introducing Eq. (7) in Eq. (2), one obtains:

$$\frac{\chi_{\parallel}(\omega, H)}{\chi_{\parallel}(0, H)} = \frac{\lambda_1 \Delta_1}{\lambda_1 + i\omega} + \frac{1 - \Delta_1}{1 + i\omega\tau_W} \tag{8}$$

The weight Δ_1 and the relaxation time, τ_W, from equation (8) can be expressed from the definitions of the integral relaxation time, τ_{int} and effective relaxation time, τ_{eff}, [9]:

$$\tau_{\text{int}} = \int_0^\infty C_{\parallel}(t,H)\,dt \tag{9}$$

$$\frac{1}{\tau_{eff}} = -\left.\frac{dC_{\parallel}(t,H)}{dt}\right|_{t=0} \tag{10}$$

Making use of Eq. (7) into Eqs. (9) and (10), one gets:

$$\Delta_1 = \frac{\tau_{\text{int}}/\tau_{eff} - 1}{\lambda_1\tau_{\text{int}} - 2 + 1/(\lambda_1\tau_{eff})} \tag{11}$$

$$\tau_W = \frac{\lambda_1\tau_{\text{int}} - 1}{\lambda_1 - 1/\tau_{eff}} \tag{12}$$

τ_{int} may be expressed by means of the averaged Legendre polynomials of the polar angle cosines corresponding to the magnetic moment of the particle, in a form similar to that of Ref. [9], with

$$\tau_{\text{int}} = \frac{6\tau_N}{Z\left(2\langle P_2\rangle_0 + 1 - 3\langle P_1\rangle_0^2\right)}\int_{-1}^{1}\left[\int_{-1}^{z}\left(y - \langle P_1\rangle_0\right)\exp\left(\sigma y^2 + \xi y\right)dy\right]^2 \frac{\exp\left(-\sigma x^2 - \xi x\right)}{1 - z^2}\,dz \tag{13}$$

where

$$\tau_N = \frac{\left(1+\alpha^2\right)vM_S}{2\alpha\gamma k_B T} \tag{14}$$

is the free Brownian motion diffusion time of the magnetic moment, α is the Landau-Lifshitz damping parameter and γ is the gyromagnetic ratio (including the spectroscopic splitting factor, g, i.e. $\gamma = g \cdot 8.79 \cdot 10^{10} s^{-1} T^{-1}$).

τ_{eff}, expressed in terms of averaged Legendre polynomials of the polar angle cosines, is given by [6], [9]:

$$\tau_{eff} = \tau_N \frac{2\langle P_2 \rangle_0 + 1 - 3\langle P_1 \rangle_0^2}{1 - \langle P_2 \rangle_0} \tag{15}$$

Thus $\chi_{\parallel}(\omega, H)$ (Eq. (8)) can be computed by means of equations (11) and (12), in which τ_{int}, τ_{eff} and λ_1 must be firstly computed.

In the low barrier case ($\sigma < 1$) and small ξ, λ_1 can be written in the form of Eq. (16) [1], [3], whilst in the high barrier case ($\sigma \geq 2$) and $h \leq 0.4$, λ_1 is given by Eq. (17) [3], [10], where

$$\lambda_1 \cong \frac{1}{\tau_N}\left(1 - \frac{2}{5}\sigma + \frac{48}{875}\sigma^2 + \frac{1}{10}\xi^2\right) \tag{16}$$

$$\lambda_1 \cong \frac{\sigma^{3/2}\left(1-h^2\right)}{\tau_N \sqrt{\pi}}\left\{(1+h)\exp\left[-\sigma(1+h)^2\right] + (1-h)\exp\left[-\sigma(1-h)^2\right]\right\} \tag{17}$$

For other situations, the eigenvalue λ_1 can be numerically computed. The method is based on the infinite hierarchy of recurrence equations for the appropriate equilibrium correlation functions [2].

For values of $h > 1$, the free energy density of a single domain particle no longer has a double-well shape and thus only the intra-well relaxation processes are possible. In this case, $\lambda_1 \to 0$ and in equation (12), the intra-well relaxation time is approximately equal to the effective relaxation time ($\tau_W \cong \tau_{eff}$). Consequently, equation (8) becomes

$$\frac{\chi_{\parallel}(\omega,H)}{\chi_{\parallel}(0,H)} \cong \frac{1}{1+i\omega\tau_{eff}} \tag{18}$$

with τ_{eff} given by Eq. (15).

The frequency and polarising field dependence of $\chi_{\perp}(\omega,H)$, is given by [6]:

$$\chi_{\perp}(\omega,H) = \chi_{\perp}(0)\frac{|\lambda|^2 + i\omega\tau_N\lambda'}{|\lambda|^2 - \omega^2\tau_N^2 + 2i\omega\tau_N\lambda'} \tag{19}$$

where

$$\chi_{\perp}(0) = \frac{v^2 M_S^2 n}{3k_B T}\left(1-\langle P_2\rangle_0\right) \tag{20}$$

is the transverse static susceptibility and

$$\lambda = \lambda' + i\lambda'' = \frac{2+\langle P_2\rangle_0}{2\left(1-\langle P_2\rangle_0\right)} + i\frac{3\langle P_1\rangle_0}{2\alpha\left(1-\langle P_2\rangle_0\right)} \tag{21}$$

is the transverse effective eigenvalue.

3. Experimental results

3.1. *Sample*

The magnetic particles of the magnetic fluid were obtained by coprecipitation of bivalent and trivalent iron ions, in aqueous solution, as described in Refs. [11] and [12]. The stabilization of the magnetic particles was done by hydrofobization with oleic acid in the absence of the carrier liquid, at a temperature of 75ºC - 80ºC, followed by a thermal treatment at 97ºC for one and a half hours. The particles were then dispersed in kerosene and further water evaporation was achieved by heating slightly above 100ºC. The resulting magnetic fluid was filtered in a magnetic field gradient, through a filamentary matrix, consisting of steel wires of approximately 17 μm in diameter.

3.2. *Compositional characterization*

In order to obtain compositional information on the magnetic material of the colloidal particles, a small amount of the magnetic fluid was mixed with acetone. The settled particles were filtered and dried in air, at room temperature. The Mo-Kα X-ray diffraction pattern of the dried particles is presented in figure 1.

According to the FCPDS-ICDD PDF-2 data base [13], the X-ray diffraction pattern of the sample displays the characteristic peaks of magnetite. Besides the peaks attributed to magnetite, the broad peak around 2θ = 6 degrees is the envelope of several peaks corresponding to the tetragonal phase of γ-Fe_2O_3 [13]. Furthermore, the broad peak corresponding to the values of 2θ ranging from 11 to 13 degrees is the envelope of a number of peaks related to the tetragonal phase of γ-Fe_2O_3 [13]. In addition, the small peak at 2θ = 22.4 degrees corresponds also to the tetragonal phase of γ-Fe_2O_3 [13].

Due to the fact that the characteristic peaks of the tetragonal phase of maghemite are not well defined, we can assert that the maghemite particles have small sizes and therefore a low degree of crystallinity.

The average size of the crystalline domains, d, of the magnetite particles can be computed from the peak corresponding to 2θ = 27.6 degrees, which includes contribution only from magnetite [13] (see figure 1). Using the Debye-Scherrer formula [14],

$$d = \frac{0.89\lambda}{\beta \cos(\theta)} \tag{22}$$

one obtains d = 7.7 nm, where λ is the X-ray wavelength of Mo-Kα (λ = 0.07093 nm), β is the full width at half maximum in radians and θ is the Bragg angle.

3.3. *Magnetic measurements*

Quasi-static magnetic measurements were carried out at 50 Hz, by means of an induction hysteresisgraph described elsewhere [15] using a 16 bit resolution card (DT 9816A, Data Translation Inc.) for analogical to digital conversion and data acquisition. The result presented in Fig.2 shows no hysteresis.

Measurements of the frequency and polarising field dependent complex magnetic susceptibility of the magnetic fluid sample, in the frequency range 0.1 – 6 GHz and over the polarising field range of 0 – 168.4 kA/m were performed by means of the transmission line technique [16] and the results are given in Figs. 3 (a) and 3 (b). For the measurements, a coaxial cell with 3 mm inner diameter and 7 mm outer diameter was used in conjunction with a HP 8753C network analyzer. The polarising field, H, was applied perpendicular to the axis of the coaxial cell, so the resulting magnetic susceptibility was a combined effect of the parallel and perpendicular components with respect to the polarising field direction.

From figure 3(b) one can observe that the maximum of the unpolarised absorption peak occurs at $f_{max\ 1}$ = 1.5 GHz, and with increasing H, a subsidiary loss peak appears at approximately f_{sub} = 1.7 GHz and that it remains distinct from the resonance peak, even in strong polarising fields of 168.4 kA/m. As previously reported [5], in the case of the ferromagnetic resonance phenomenon, the real part of the complex magnetic susceptibility is zero at the resonance frequency, f_{res} (going from a positive to a negative value). Both f_{res} and the frequency corresponding to the ferromagnetic resonance peak, f_{max} increase linearly with increasing H [5]. Unlike the typical behaviour of the complex magnetic susceptibility at resonance, the frequency of the subsidiary peak remains practically unchanged and the real part of the complex magnetic susceptibility does not go through zero. Therefore, the subsidiary loss peak is considered to be a relaxation peak.

As shown in Ref. [5], for $H>H_A$, equation (23) is applicable, where M_S is expressed in Tesla.

$$f_{res} = \frac{\gamma\left(1+\alpha^2\right)^{1/2}}{2\pi}\left(H + \frac{2K}{M_S}\right) \tag{23}$$

Fig. 4 shows a plot of a straight line dependence of f_{res} against H for the sample, with the intercept of the H-axis occurring at H = -53.57 kA/m. The absolute value of the intercept corresponds to the effective value of the anisotropy field of the particles, H_A = 53.57 kA/m [5].

Making use of the value of spontaneous magnetization of magnetite [17], $M_S(magnetite)$ = 0.6 Tesla and of the value of the magnetocrystalline anisotropy constant of magnetite [18], $K(magnetite) = 1.1 \cdot 10^4\ Jm^{-3}$, one gets the anisotropy field, $H_A(magnetite) = \frac{2K(magnetite)}{M_S(magnetite)} = 36.6 kA/m$. This value is much smaller than that obtained from Fig. 4, of H_A = 53.57 kA/m. This means that the magnetic fluid sample contains particles with an anisotropy field larger than that of magnetite and these can only be particles of the tetragonal phase of maghemite. This conclusion is supported by the results of the X-ray diffraction analysis.

4. Theoretical results

In this section we investigate theoretically the conditions which may give rise to the subsidiary relaxation peak, observed in Fig. 3(b), by taking into account the characteristics of our magnetic fluid sample. In so doing, we test the validity of the theoretical model and we also reveal the origin of the subsidiary relaxation peak (by determining if it is due to magnetite particles or to the particles of the tetragonal phase of maghemite).

Due to the fact that in our sample, two types of particles exist, it is not possible to determine experimentally the particle size distribution and the particle concentration of each type of magnetic particles. Consequently, in the following analysis, we do not take into account a specific particle concentration and therefore, the plots will be normalized to $\chi(0,H)$.

In the first theoretical situation (TS1 of Fig. 5), we consider the case of the overall complex magnetic susceptibility (Eq. (1)) of a sample which only consists of magnetite single domain particles. The computations were made as described in section 2. For the computations, the following parameters were used: $M_S(magnetite)$ = 0.6 Tesla [17], $K(magnetite) = 1.1 \cdot 10^4$ Jm^{-3} [18], α = 0.1, H = 168.4 kA/m and T = 300 K. In figure 5 is presented a normalized plot of $\chi''(f,H)$ of a magnetite single domain particle system, for various particle diameters. The inset figure is a magnification of the data over the

frequency interval, where we have experimental results of the magnetic fluid sample (0.1 to 6 GHz).

From figure 5 one can observe that apart from the ferromagnetic resonance peaks in the frequency range 6 to 7 GHz, the magnetite particles with diameters of 5 nm and 6 nm (curves 2 and 3) give rise to loss peaks at 1.1 GHz and 1 GHz, which differ from the experimental frequency of the subsidiary relaxation peak of approximately 1.7 GHz (see Fig. 3 (b)).

From Eqs. (4), (5), (14) and (15) one can see that the larger the damping parameter α, the smaller the effective relaxation time, τ_{eff} . As discussed in section 2, for values of $h > 1$, the intrawell relaxation time is approximately equal to the effective relaxation time ($\tau_W \cong \tau_{eff}$) and therefore, the increase of the damping parameter, α, leads to an increase of the frequency corresponding to the intra-well relaxation peak in a strong polarizing field.

Consequently, in trying to determine if the magnetite particles were responsible for the occurrence of the subsidiary peak at 1.7 GHz, we analyzed another theoretical situation, denoted by TS2. In TS2, apart from a damping parameter of $\alpha = 0.15$, the same parameters as used in TS1 were used. The results are given in Fig. 6.

One can observe that increasing the damping parameter from 0.1 to 0.15, the relaxation peaks which were visible in the theoretical situation TS1 (curves 2 and 3 in Fig. 5) became shoulders in the case of TS2 (curves 2 and 3 in Fig. 6). Therefore, by increasing the damping parameter one cannot get a well defined relaxation peak of magnetite particles; at the frequency of 1.7 GHz (see Fig. 3 (b)).

Now, returning to the TS1 situation, it is true that the magnetite particles with diameters of 5 nm and 6 nm (curves 2 and 3 in Fig. 5) give rise to loss peaks at frequencies around 1 GHz, but if we compare the amplitude of the resonance absorption peak with the amplitude of the intra-well relaxation peak and we also take into account the experimental average crystallite diameter of magnetite particles of the order of 7.7 nm (as determined in section III.B), we may conclude that magnetite particles make only a small contribution to the measured relaxation peak.

Little is reported in the literature on the experimental value for the magnetocrystalline anisotropy constant, K, of the tetragonal phase of maghemite, because

usually no correlation was made between the measured values of K and the crystalline structure of maghemite (i.e. cubic phase or tetragonal phase). In Ref. [19] a value of $2.3 \cdot 10^5$ J/m^3 has been reported for K of maghemite particles. Due to the fact that this value is much larger than the K value of bulk cubic maghemite, $4.7 \cdot 10^3$ J/m^3 [20], one may presume that it corresponds to the tetragonal phase of maghemite. Similar large K values for maghemite were reported in Refs. [21-23].

In the third theoretical situation TS3, we computed the overall complex magnetic susceptibility of a sample consisting only of maghemite single domain particles. For the computations the following parameters, M_S*(maghemite)* = 0.524 Tesla [24], *K(maghemite)* = $2.3 \cdot 10^5$ J/m^3 [19], α=*0.2*, H = 168.4 kA/m and T = 300 K, were used. The results are presented in figure 7, for various particle diameters.

Thus, in the case of TS3, in which for the particles of the tetragonal phase of maghemite a K of $2.3 \cdot 10^5$ J/m^3 was assumed, a prominent intra-well relaxation peak is visible around 1.7 GHz for a particle diameter of 4 nm. Also, in this case the intra-well relaxation peak is clearly visible and distinct from the resonance peak, unlike the other situations of TS1 and TS2. Based on these theoretical results, we conclude that small maghemite particles contribute to the measured relaxation peak.

Due to the fact that our magnetic fluid consists of magnetite and maghemite particles and it is not possible to determine experimentally the particle size distribution of each type of magnetic particles, any further theoretical analyses involving an assumed proportion of magnetite in a theoretical mixture, or based on an assumed particle size distribution, would be of a rather speculative character. However, some concluding remarks may be drawn.

The theoretical situation TS1 showed that the magnetite particles with diameters of 5 nm and 6 nm and damping parameter α =0.1 contribute to a relaxation peak around the frequency of 1 GHz. By increasing the damping parameter to get a relaxation peak at higher frequency (as we have measured), the peaks become shoulders of the resonance absorption peak (see Fig. 6 of the theoretical situation TS2).

Bearing in mind that the typical average diameter or magnetite particles in magnetic fluids is 10 nm, it now becomes clear why in such magnetic fluids the intra-well relaxation process is manifested at most as a shoulder of the ferromagnetic resonance

absorption peak [5-7] (i.e. due to small size particles, with diameter of 5 – 6 nm, whose contribution to the susceptibility depends on the particle size distribution in the sample).

Making a comparison between the theoretical situations TS2 and TS3, we can assert that for samples consisting of particles with a large magnetocrystalline anisotropy constant (those in TS3), the frequency gap between the frequency corresponding to the intra-well relaxation peak and the frequency of the ferromagnetic resonance peak is large enough to make the intra-well relaxation peak distinct from the resonance peak.

The X-ray diffraction analysis presented in section 3.2 revealed that the magnetite particles within the sample have an average diameter of 7.7 nm. Also, due to the fact that the characteristic peaks of the tetragonal phase of maghemite are not well defined and instead of distinct peaks, the XRD pattern presents broad peaks, we conclude that the maghemite particles are small in size. Taking into account these experimental facts and the theoretical results (TS1, TS2 and TS3) we conclude that the subsidiary loss peak measured on the investigated magnetic fluid sample in strong polarising fields is mainly due to the intra-well relaxation process of small particles of the tetragonal phase of maghemite.

5. Conclusions

A kerosene-based magnetic fluid with two types of iron oxides particles, stabilized with oleic acid has been investigated.

The XRD analysis shows that the investigated sample contains magnetite particles together with particles of the tetragonal phase of maghemite. The anisotropy field results show that the anisotropy field of the investigated sample is much larger than the value corresponding to magnetite alone, supporting thus the results of the XRD analysis.

Unlike other magnetic fluids in which the intra-well relaxation process is manifested as a shoulder of the ferromagnetic resonance peak, the sample investigated here presents a clear subsidiary loss peak in strong polarising field. The shift in the frequency corresponding to the subsidiary peak does not obey the typical behaviour of ferromagnetic resonance and although the amplitude of the subsidiary peak decreases with the increasing polarising field, the peak remains distinct and does not vanish, even in polarising fields of 168.4 kA/m.

The theoretical analysis (in which we have taken into account the characteristics of our sample) has revealed that the subsidiary peak of the investigated sample is due to the intra-well relaxation process of the small particles of the tetragonal phase of maghemite.

The results confirm the work of Coffey and co-workers who published the first theoretical papers on the intra-well relaxation process, confirming thus the validity of their theory.

Acknowledgements

This work was supported in part by CNMP grant no. 1-32155/2008. P. C. Fannin acknowledges ESA for part funding of this work. Acknowledgement is also due to L. Gabor for manufacturing the magnetic fluids and C. Couper for assistance provided.

References

[1] W. F. Brown, Phys. Rev. 130 (1963) 1677.

[2] W. T. Coffey, D. S. F. Crothers, Yu. P. Kalmykov and J. T. Waldron, Phys. Rev. B 51 (1995) 15947.

[3] D. A. Garanin, Phys. Rev. E 54 (1996) 3250.

[4] P. C. Fannin, L. Kinsella and S. W. Charles, J. Phys. D: Appl. Phys. 30 (1997) 2292.

[5] P. C. Fannin, C. N. Marin and I. Malaescu, J. Phys.: Condensed Matter 15 (2003) 4739.

[6] P. C. Fannin, Yu. P. Kalmykov and S. W. Charles, J. Magn. Magn. Mater. 289 (2005) 133.

[7] P. C. Fannin and C. N. Marin, J. Magn. Magn. Mater. 299 (2006) 425.

[8] Yu. L. Raikher and M. I. Shliomis, Adv.Chem.Phys., *Relaxation Phenomena in Condensed Matter*, vol. 87, ch.8 (1994) 595.

[9] Yu. P. Kalmykov, W. T. Coffey and S. V. Titov, J. Magn. Magn. Mater. 265 (2003) 44.

[10] A. Aharoni, Phys. Rev. 177 (1969) 793.

[11] I. Malaescu, L. Gabor, F. Claici and N. Stefu, J. Magn. Magn. Mater. 222 (2000) 8.

[12] I. Hrianca, L. Gabor, I. Malaescu, A. Ercuta and F. Claici, Romanian Reports in Physics 47 (1995) 821.

[13] JCPDS - *International Centre for Diffraction Data, PDF-2 Data Base* 1999.

[14] H. P. Klug and L. E. Alexander, *X-Ray Diffraction Procedures for Polycrystalline and Amorphous Materials*, 2nd edition, John Wiley & Sons 1974.

[15] I. Mihalca and A. Ercuta, *Journal of Optoelectronics and Advanced Materials*, 5 (2003) 245.

[16] P. C. Fannin, C. MacOireachtaigh and C. Couper, J. Magn. Magn. Mater. 322 (2010) 2428.

[17] E. Kneller, *Ferromagnetismus,* Springer-Verlag, Berlin 1962.

[18] L. R. Bickford, Phys. Rev. 78 (1950) 449.

[19] P. Dutta, A. Manivannan, M. S. Seehra, N. Shah and G. P. Huffman, Phys. Rev. B 70 (2004) 174428.

[20] G. Bate, *Magnetic Oxides*, ed. D. J. Craik, Wiley, London 1975.

[21] E. Mosiniewicz-Szablewska, M. Safarikova and I. Safarik, J. Phys. D: Appl. Phys. 40 (2007) 6490.

[22] B. Martínez, A. Roig, E. Molins, T. González-Carreño and C. J. Serna, J. Appl. Phys. 83 (1998) 3256.

[23] Y. Komorida, M. Mito, H. Deguchi, S. Takagi, A. Millán, N. J. O. Silva and F. Palacio, Appl. Phys. Lett. 94 (2009) 202503.

[24] R**.** Hergt, R. Hiergeist, I. Hilger, W. A. Kaiser, Y. Lapatnikov, S. Margel and U. Richter, J. Magn. Magn. Mater. 270 (2004) 345.

Figure captions

Fig.1. X-ray diffraction pattern (Mo-Kα) of the magnetic powder as obtained by flocculation with acetone

Fig.2. Quasi-static magnetization curve of the investigated magnetic fluid

Fig.3. Frequency and polarising field dependence of the complex magnetic susceptibility of the investigated sample over the frequency range 0.1 to 6 GHz: (a) the real part, $\chi'(\omega, H)$ and (b) the imaginary part $\chi''(\omega, H)$. The values of the polarising field are: 1 – 0, 2 - 15.2 kA/m, 3 - 24.9 kA/m, 4 - 35.6 kA/m, 5 - 45.8 kA/m, 6 - 56.8 kA/m, 7 - 69.1 kA/m, 8 - 80.3 kA/m, 9 - 91.1 kA/m, 10 - 102.4 kA/m, 11 - 114.1 kA/m, 12 - 124.7 kA/m, 13 - 135.4 kA/m, 14 - 147.2 kA/m, 15 - 158.3 kA/m, 16 - 168.4 kA/m.

Fig.4. Polarising field dependence of the resonance frequency of the investigated magnetic fluid

Fig.5. Theoretical normalized plots of $\chi''(f, H)$ for various particle diameters (TS1)

Fig.6. Theoretical normalized plots of $\chi''(f, H)$ for various particle diameters (TS2)

Fig.7. Theoretical normalized plots of $\chi''(f, H)$ for various particle diameters (TS3)

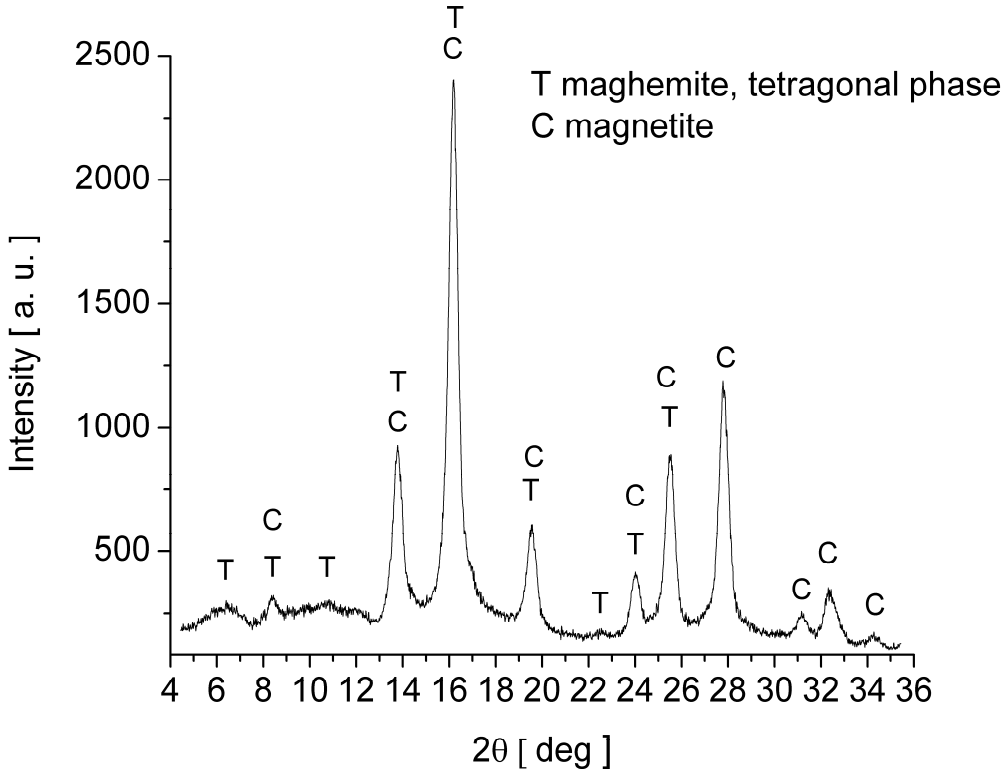

Fig. 1

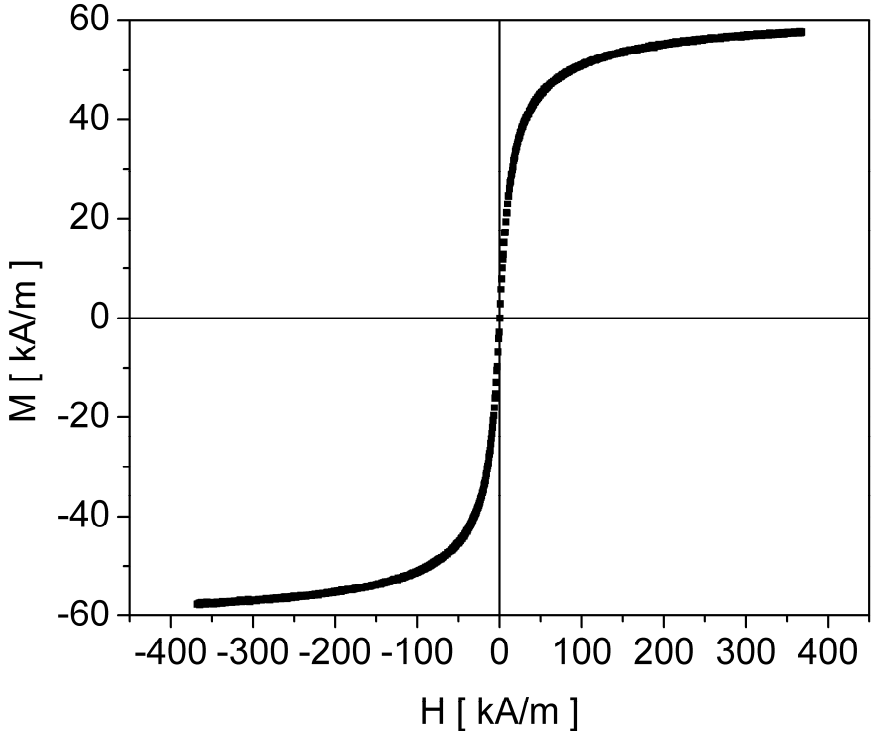

Fig. 2

Fig. 3a

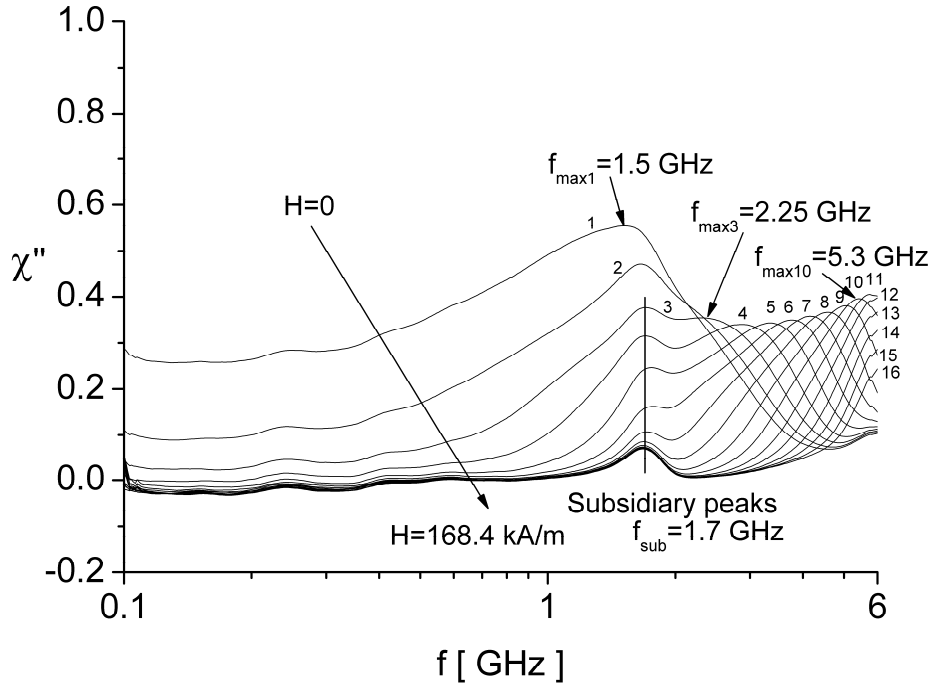
1.0
0.8
0.6
0.4
0.2
0.0
-0.2
χ"
0.1
1
6
f [GHz]
H=0
f_max1=1.5 GHz
f_max3=2.25 GHz
f_max10=5.3 GHz
1
2
3
4
5 6 7 8 9 10 11
12
13
14
15
16
Subsidiary peaks
H=168.4 kA/m
f_sub=1.7 GHz

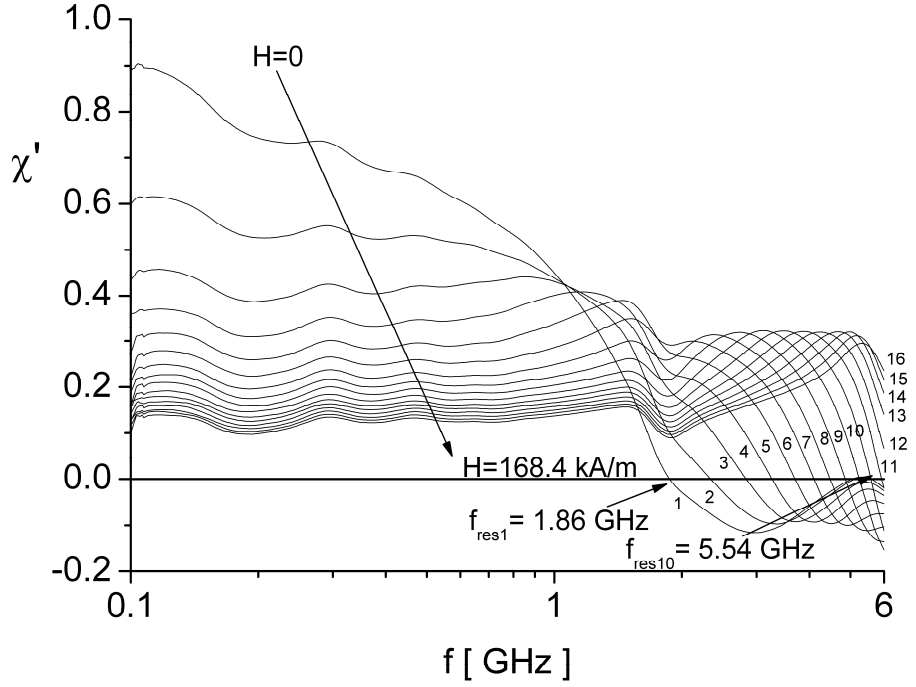
1.0
0.8
0.6
0.4
0.2
0.0
-0.2
χ'
0.1
1
6
f [GHz]
H=0
16
15
14
13
12
11
10
9
8
7
6
5
4
3
2
1
H=168.4 kA/m
f_res1= 1.86 GHz
f_res10= 5.54 GHz

Fig. 3b

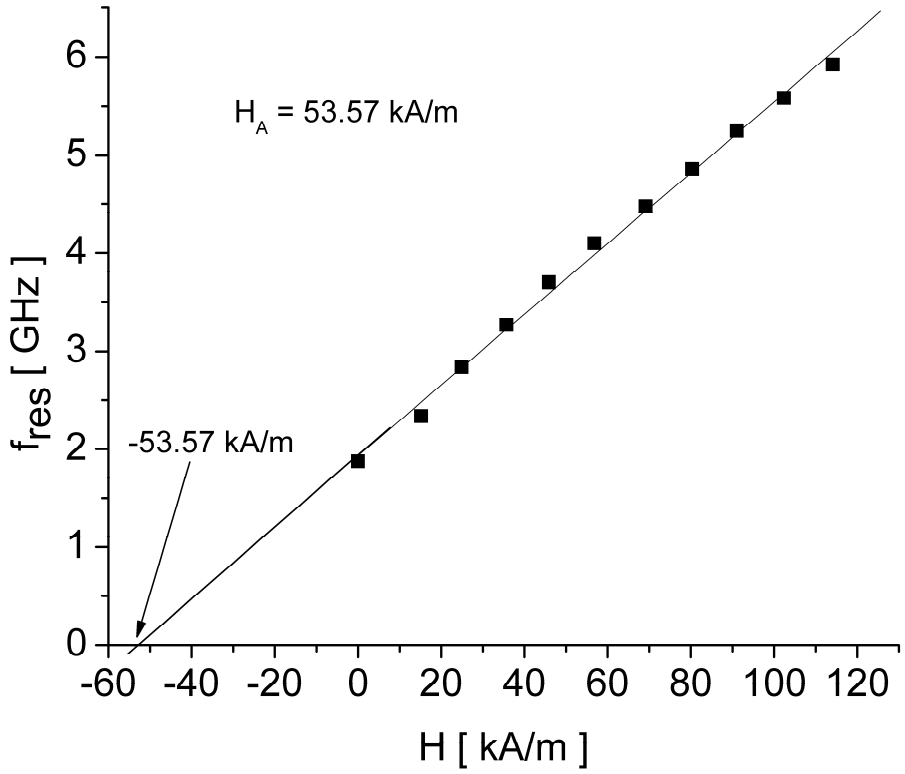

Fig. 4

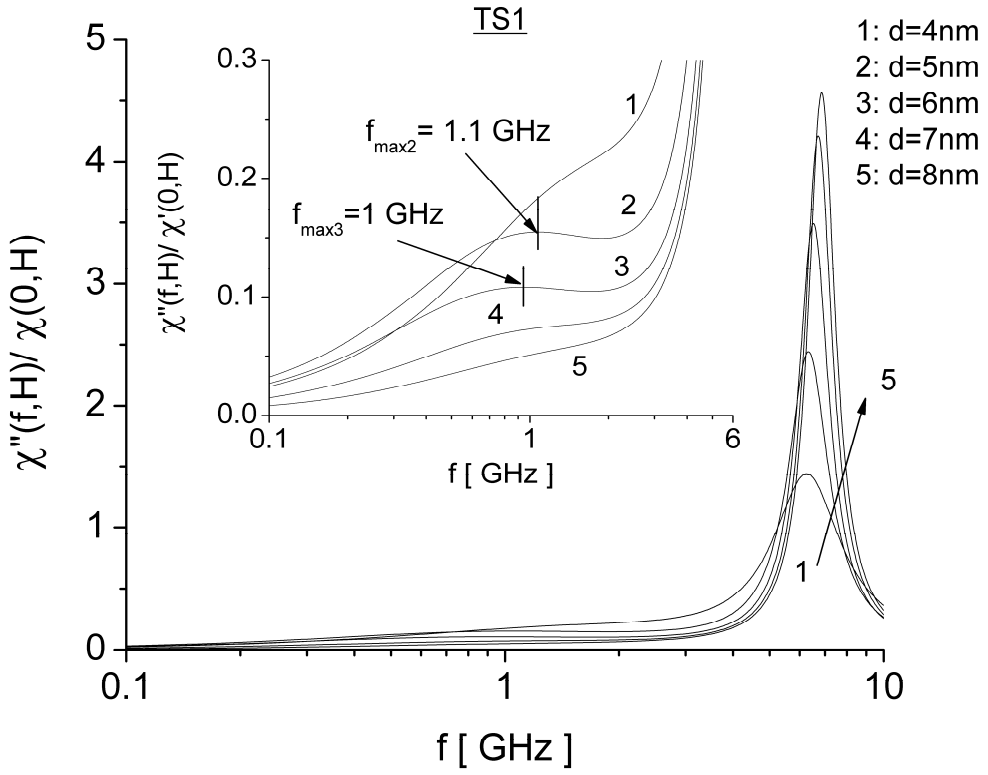

Fig. 5

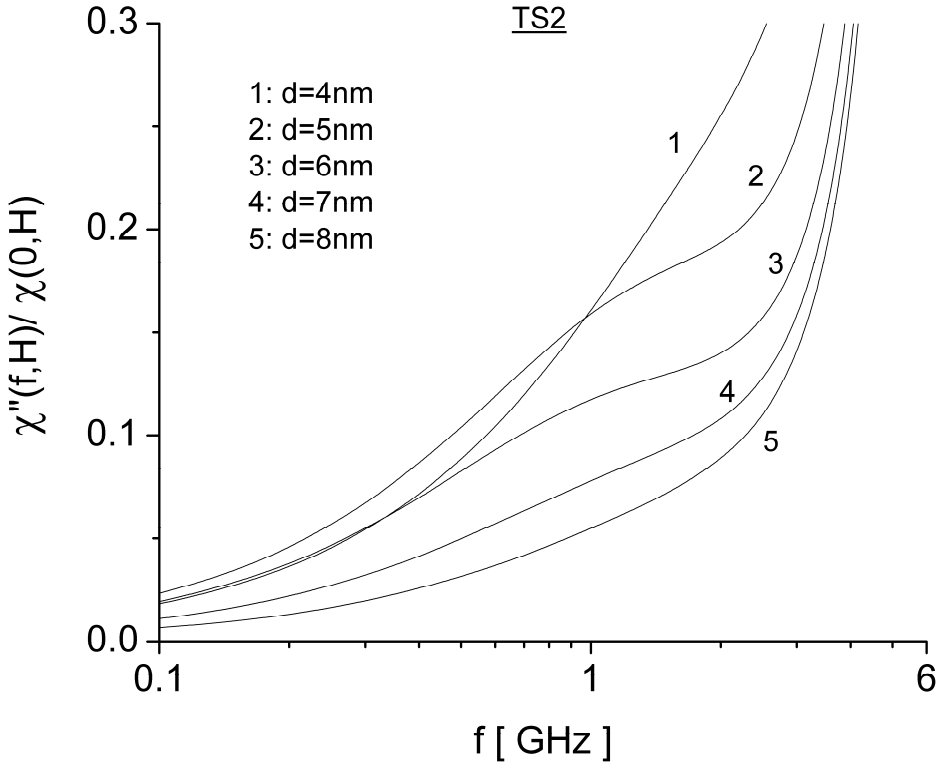

Fig. 6

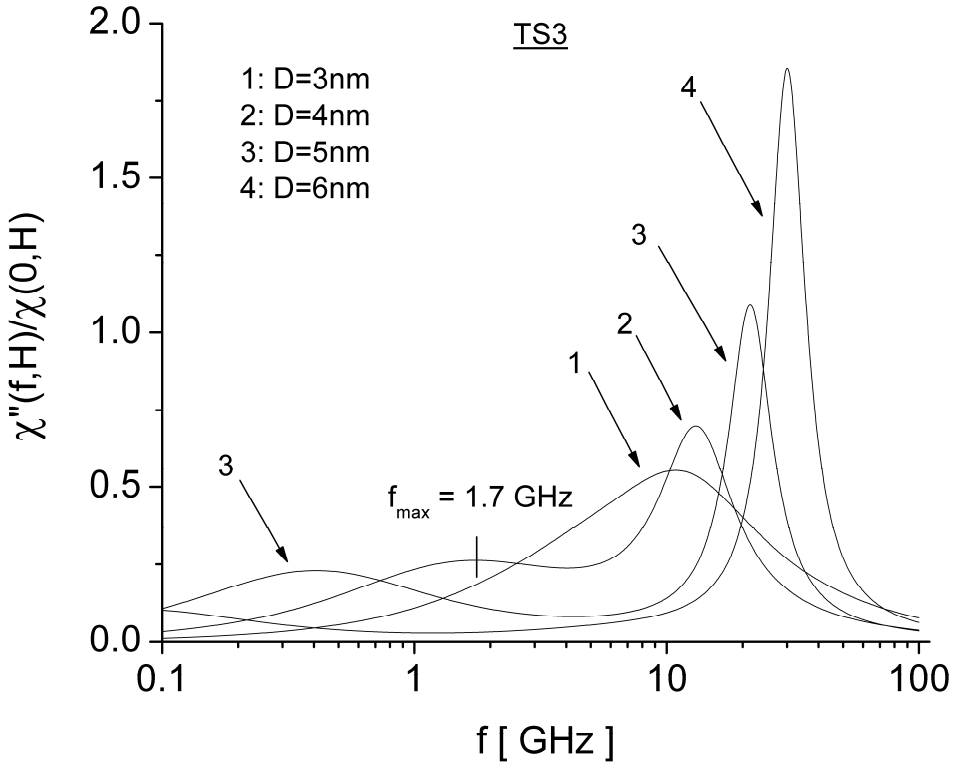

Fig. 7

>The intra-well relaxation process in a magnetic fluid is studied.
>The sample consists of the tetragonal phase of maghemite and magnetite particles.
>A subsidiary relaxation peak is observed in the vicinity of the resonance peak.
>The relaxation peak is correlated to the intra-well relaxation process.
>It is assigned to the tetragonal phase of maghemite particles.